t_1-Noise Elimination by Continuous Chemical Shift Anisotropy Refocusing

Frédéric A. Perras,[a]* Tian Wei Goh,[a,b] Wenyu Huang[a,b]
[a]US DOE, Ames Laboratory, Ames, IA 50011, USA
[b]Department of Chemistry, Iowa State University, Ames, IA 50011, USA
*author to whom correspondence should be addressed, fperras@ameslab.gov

Highlights

- The refocusing of chemical shift anisotropy during heteronuclear dipolar recoupling improves the stability of the sequence
- One way to achieve this is by adding windows where simultaneous inversion pulses can be applied
- The same effect can also be achieved continuously in a windowless sequence by involving both channels
- This "CSA-free" recoupling sequence leads to higher transfer efficiencies and reduces t_1-noise in D-HMQC experiments

Abstract

Due to their high gyromagnetic ratio, there is considerable interest in measuring distances and correlations involving protons, but such measurements are compounded by the simultaneous recoupling of chemical shift anisotropy (CSA). This secondary recoupling adds additional modulations to the signal intensities that ultimately lead to t_1-noise and signal decay. Recently, Venkatesh et al. demonstrated that the addition of CSA refocusing periods during ^{1}H-X dipolar recoupling led to sequences with far higher stability and performance. Herein, we describe a related effort and develop a symmetry-based recoupling sequence that continually refocuses the ^{1}H CSA. This sequence shows superior performance to the regular and t_1-noise eliminated D-HMQC sequences in the case of spin-1/2 nuclei and comparable performance to the later for half-integer quadrupoles.

Graphical Abstract

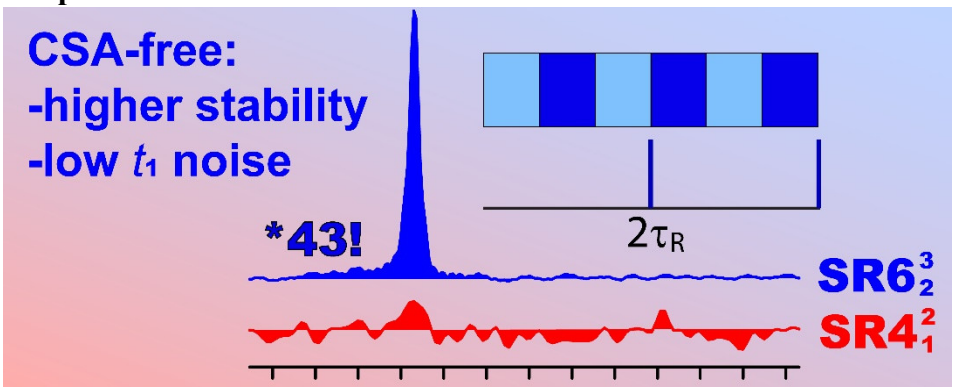

Keywords

Solid-state NMR, Dipolar recoupling, Fast magic angle spinning, D-HMQC, Chemical shift anisotropy

Introduction

Heteronuclear correlation (HETCOR) nuclear magnetic resonance (NMR) experiments are applied to reveal proximities between different sites in a material. These proximities can, in turn, be used to determine the local structure and develop structure-activity relationships. In solids, HETCOR experiments primarily use cross-polarization (CP) to transfer magnetization from one nuclide to another.[1-3] CP is highly-efficient for most light spin-1/2 nuclei, such as ^{1}H, ^{13}C, ^{15}N, ^{29}Si, and ^{31}P, and has been used to great effect in biomolecular solid-state NMR. Unfortunately, CP suffers from an offset dependence that makes it challenging to apply to heavy spin-1/2 nuclei.[4-6] Given that it relies on the spin locking of both nuclei at similar radiofrequency (rf) powers, it is challenging to apply to half-integer quadrupolar nuclei, which can typically only be spin locked with very low rf powers,[7-10] as well as low-γ nuclei, which generally have low nutation frequencies, particularly when using large diameter rotors for enhanced sensitivity.[11,12] All of these challenges have made dipolar recoupling-based HETCOR approaches increasingly attractive in materials science.[13-23]

The dipolar-heteronuclear multiple quantum coherence (D-HMQC) experiment is likely the simplest of the recoupling-based HETCOR methods.[24,15] In the D-HMQC experiment, all of the most demanding pulse sequence elements are placed on a single channel, while the other channel requires only the application of either two excitation/reconversion pulses or a Hahn echo. This simplicity enables the correlation to quadrupolar nuclei and heavy spin-1/2 nuclei with high transfer efficiencies and excitation bandwidths.[5,19,25-33]

One of the main applications of the D-HMQC sequence is for the indirect proton detection of low-sensitivity nuclei. In this case, the dipolar recoupling sequence must be applied to the proton spins for two main reasons. Firstly, the use of recoupling sequences that only reintroduce the m=2 components of the heteronuclear dipolar coupling Hamiltonian[34] enables for the simultaneous application of ^{1}H homonuclear decoupling, which is critical for obtaining coherence lifetimes of sufficient duration to form the multiple quantum coherence. Secondly, it is often impossible to efficiently apply recoupling on the indirect channel if it is a quadrupolar, low-γ, or heavy spin-1/2 nuclide. Heteronuclear dipolar coupling is, however, well known to have the same rotational signatures as chemical shift anisotropy (CSA), and as such any recoupling sequence that reintroduces the heteronuclear dipolar interactions will also reintroduce the CSA.[34] It is worth noting that certain challenging nuclei can be efficiently recoupled using the recently proposed transfer of population double-resonance (TRAPDOR) HMQC.[35,36]

The influence of ^{1}H CSA in D-HQMC experiments was ignored until very recently because it should, in theory, be refocused perfectly by the Hahn echo.[37] For the CSA to be perfectly refocused, however, the sequence requires an unreasonable nutation frequency and spinning stability (< 1 Hz). These unavoidable instabilities lead to shorter coherence lifetimes, lower transfer efficiencies, and high levels of t_1 noise. In a recent study, Venkatesh et al. showed that t_1 noise could be dramatically reduced in D-HMQC experiments if simultaneous inversion pulses were applied to both channels at the halfway points of the recoupling periods to refocus the CSA.[37] Their t_1-noise eliminated (TONE) D-HMQC sequences further enabled the addition of a purge pulse to remove uncorrelated magnetization. Although the TONE sequences require the addition

of two windows, each lasting a total of two rotor periods (t_r) during which magnetization can decay, they typically generate not only lower noise levels, but also higher coherence transfer efficiencies and signal intensities due to the longer coherence lifetimes.[38]

Results and Discussion

We were intrigued to see whether it was possible to build on the TONE concept and refocus the CSA continuously rather than only once per recoupling period. Of course, adding more windows would lead to diminishing returns, so this option was not explored. Not all heteronuclear recoupling experiments are sensitive to the CSA, however, most notably CP, which includes Brinkmann and Levitt's generalized Hartman Hahn sequences.[39] Garbow and Gullion also showed that the stability of rotational-echo double-resonance (REDOR)[40] experiments[41] could be dramatically improved if the recoupling pulses were divided between the two channels, effectively ensuring that the CSA is never recoupled. In the case of γ-encoded dipolar recoupling, it is possible to invert the sign of the recoupled dipolar precession frequency by simply inverting the phase of the recoupling sequence.[34] Applying this phase shift simultaneously to the application of an inversion pulse on the second channel provides a convenient, windowless, approach to refocusing the CSA.[14,42,43] Ideally, we would want to transfer this concept to zero-quantum, non-γ-encoded, heteronuclear dipolar recoupling. Phase shifts, however, do not affect the sign of the recoupled dipolar frequency for such sequences.

The idea then was to search for a recoupling sequence that decoupled all anisotropic interactions over a complete cycle, lasting $2t_r$, but that would have non-zero scaling factors for the zero-quantum heteronuclear terms after a single rotor cycle. The sequence would thus take the form RN_2^{ν}.[34,44,45] It then goes to reason that if the scaling factor for the zero-quantum heteronuclear dipolar coupling terms is κ after the first rotor period, then is it necessarily -κ during the second. If an inversion pulse is applied to the second channel each rotor period, this would preserve the sign of the recoupled dipolar interactions and, much like γ-encoded sequences, enable the windowless refocusing of CSA terms while recoupling the heteronuclear dipolar terms. Note that the sequence cannot have non-zero γ-encoded heteronuclear terms, even after the first rotor period; otherwise, they will also evolve and lead to decoherence.

We were able to identify a single sequence that fit the criteria outlined in the previous paragraph. This sequence, $\mathrm{R6}_2^3$, shown in Figure 1, features a 180° phase shift, much like the popular $\mathrm{R4}_1^2$ sequence,[46,47] which makes it insensitive to rf maladjustments, but more crucially eliminates all non-zero-quantum heteronuclear dipolar coupling terms at each rotor period. Throughout its full 2-rotor cycle, it recouples only the isotropic chemical shift and *J* coupling terms. During the first rotor period, however, it recouples both the *m*=1 and 2 zero-quantum heteronuclear terms with scaling factors of 0.147 and 0.149, respectively, if a 180_0 pulse is used as the basic *R* element. We will refer to this approach as CSA-free heteronuclear dipolar recoupling. While $\mathrm{R4}_1^2$ has a larger scaling factor of 0.204, it only recouples the m=2 terms, and as a result, the two sequences yield similar buildup rates. We will be applying the same $\mathrm{SRN}_n^{\nu} = (\mathrm{RN}_n^{\nu}\mathrm{RN}_n^{-\nu})3^1$ supercycle to both recoupling sequences (Figure 1d).[45-47,48-51]

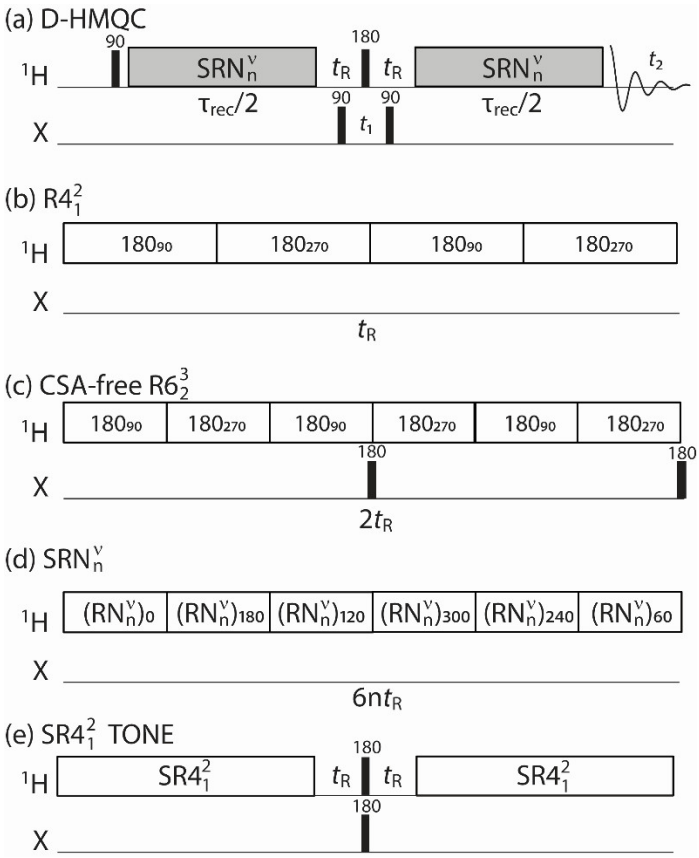

Figure 1. Diagrams of the various pulse sequences discussed in the paper. (a) Basic form of the D-HMQC sequence. The recoupling part in (a) can take multiple forms, outlined in (b)-(e). The basic $R4_1^2$ sequence is shown in (b) while the CSA-free $R6_2^3$ sequence is shown in (c) and involves pulses on both channels. These sequences are generally supercycled to $SR4_1^2$ and CSA-free $SR6_2^3$ using the supercycle described in (d). TONE recoupling splits a $SR4_1^2$ recoupling period into two with the application of simultaneous inversion pulses to both channels (e).

We first explored the performance of the various sequences *in silico* using SIMPSON[52,53] by calculating the D-HMQC transfer efficiencies as a function of MAS rate offset ($\Delta\nu_{MAS}$) and recoupling time (τ_{rec}), see Figure 2. The dipolar coupling strength was set to 500 Hz. We calculated that all three sequences ($SR4_1^2$, $SR4_1^2$ with TONE, and CSA-free $SR6_2^3$) would have similar robustness to long recoupling times and MAS instabilities if the ^{1}H CSA anisotropy parameter (δ_{aniso}) was equal to zero. As δ_{aniso} increases to 5 ppm (typical of a C-H ^{1}H) and 20 ppm (typical of an O-H ^{1}H), however, the efficiency of $SR4_1^2$ is highly compromised. This limits the application of $SR4_1^2$ to short recoupling durations (strong dipolar couplings), and even then, the sensitivity to MAS rate fluctuations will lead to significant t_1 noise.

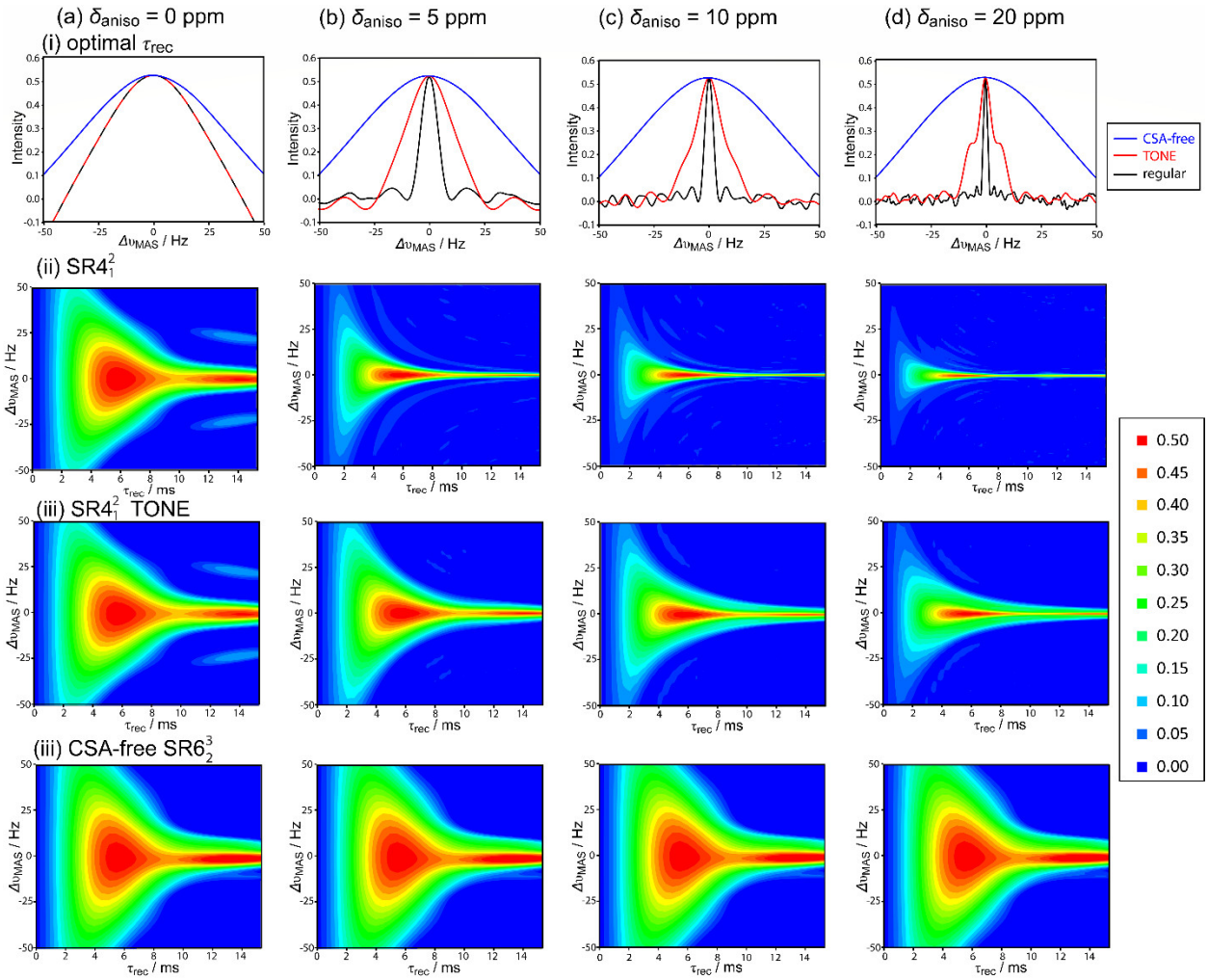

Figure 2. SIMPSON simulations of the sensitivity of $SR4_1^2$, TONE, and $SR6_2^3$ to spinning rate fluctuations. Simulations are performed for ^{1}H δ_{aniso} values of 0 (a), 5 (b), 10 (c), and 20 (d) ppm. The recoupled signal intensity as a function of MAS offset at the recoupling maximum is shown in (i). 2D plots of this intensity relative to recoupling time and MAS offset are shown in (ii)-(iv) for the three sequences, respectively. Colors represent the transfer efficiencies in accordance with the legend on the right.

The $SR4_1^2$ sequence that is enhanced with TONE fares much better than continuous $SR4_1^2$ recoupling, remaining relatively insensitive to MAS rate instabilities; however, its performance still degrades as the magnitude of the CSA increases. In contrast to these two sequences, the CSA-free $SR6_2^3$ sequence is completely unaffected by ^{1}H CSA, yielding the identical performance with δ_{aniso} = 20 ppm as 0 ppm. Its robustness to MAS rate instabilities is also aways superior to $SR4_1^2$ even with the application of TONE.

We compared the performance of the three sequences using 1D ^{1}H{^{15}N} D-HQMC in ^{15}N-enriched glycine, see Figure 3. For this sample, TONE yields 43% higher signal intensities than the unmodified $SR4_1^2$ sequence while the CSA-free $SR6_2^3$ sequence yields over twice the transfer efficiency. Oscillations in the TONE build-up curve in Figure 3a are caused by incomplete

supercycling. The difference is particularly drastic in the case of the methylene ^{1}H spins given that the dipolar coupling to ^{15}N is weaker and thus requires longer recoupling times. In this case, only TONE and the CSA-free sequence are seen to lead to significant transfer efficiencies, with the two having nearly equal performances. None of the 2D spectra measured on this sample contained any t_1 noise; they are available on Zenodo.

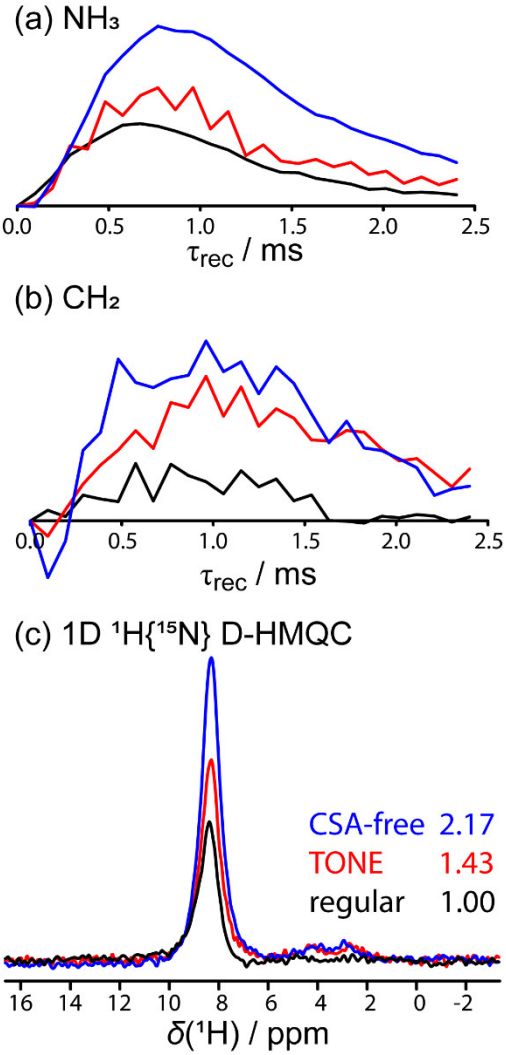

Figure 3. Relative performance of $SR4_1^2$ (black), $SR4_1^2$ with TONE (red), and CSA-free $SR6_2^3$ (blue) D-HMQC sequences on ^{15}N-labelled glycine at 83.333 kHz MAS. The intensity of the recoupled NH_3 signal is shown in (a) and the CH_2 signal is shown in (b). The 1D spectra at the recoupling times offering the maximum intensities are shown in (c).

At this point, it is worth mentioning the sensitivity of the CSA-free sequence to ^{15}N rf pulse imperfections. The experiments shown in Figure 3 were performed with an MAS rate of 83.333 kHz meaning that a ^{15}N inversion pulse is applied every 12 µs. After 2.5 ms of recoupling, we would have thus applied over 200 ^{15}N inversion pulses. If they are not supercycled, we do not see the generation of significant D-HMQC signals. We trialed the XY8,[54] XY16,[54] $XY4_4^1$,[55] MLEV16,[56] and 0013[57] supercycles, however, none of these provided good efficiencies at

incomplete supercycles or long recoupling times. We obtained the best performance using Manu and Veglia's computer-optimized GAN supercycles.[58] We found, however, that a simple $x\bar{x}\bar{x}x$ supercycle was able to match the performance of the GAN supercycles and thus it was used throughout. Surprisingly the longer $x\bar{x}\bar{x}x\ \bar{x}xx\bar{x}$ supercycle was found to have a lower performance to the shorter $x\bar{x}\bar{x}x$ supercycle. This supercycle does not seem to have been discussed in the context other similar Carr-Purcell type recoupling sequences, such as REDOR, where it may very well lead to a higher performance than the currently-used XY-type cycles.

Given that the primary benefits of the sequence are seen for lower-frequency nuclei and sites with weak dipolar couplings that require longer recoupling times, we tested the performance of the sequence on the proton-detection of ^{89}Y in the metal-organic framework: Y-MOF-76.[59-61] Figure 4a shows the build-up of the multiple quantum coherences using all three sequences. As expected, the three sequences perform similarly at short recoupling times where the MAS rate sensitivity is low. As the recoupling times increase, however, the TONE sequence is able to sustain the recoupling for longer, leading to 2.32 times higher signal intensities, with the CSA-free sequence yielding further improved efficiency, with 3.23 times higher signal intensities (Figure 4b). We can observe some small oscillations in the build-up curve for the CSA-free sequence in Figure 4a, blue. These are caused by the incomplete ^{89}Y supercycle. The increments were set to 6 rotor period for each of the recoupling blocks as this is the total duration of the $SR6_2^3$ sequence, but the ^{89}Y supercycle lasts only 4 rotor periods.

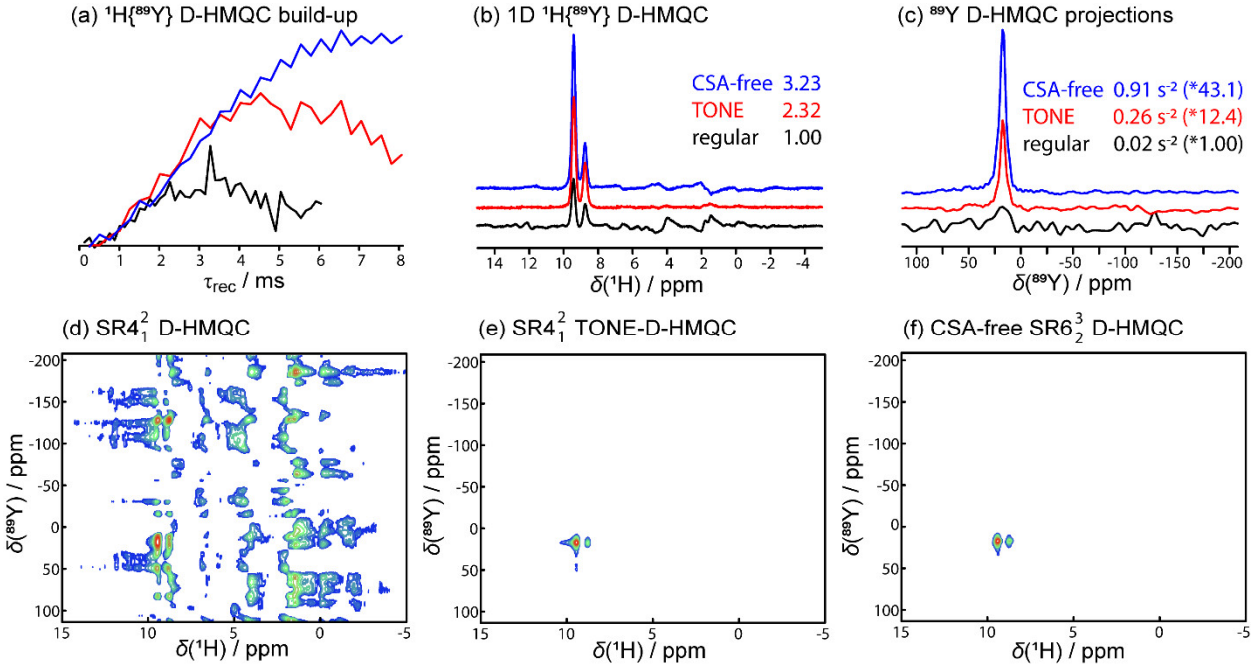

Figure 4. Relative performance of $SR4_1^2$ (black), $SR4_1^2$ with TONE (red), and CSA-free $SR6_2^3$ (blue) D-HMQC sequences in ^{1}H{^{89}Y} D-HMQC on Y-MOF-76. The MAS rate was 47.619 kHz. The buildup of signal is shown in (a). The multiple-quantum-filtered ^{1}H NMR spectra at the optimal recoupling times are shown in (b). The indirectly-detected ^{89}Y NMR spectra are shown in (c), while the 2D spectra are shown in (d)-(f).

If we perform two-dimensional acquisitions, the performance gaps between the sequences further widen. The unmodified $SR4_1^2$ sequence leads to tremendous t_1 noise and a barely distinguishable signal. With TONE, however, the t_1 noise is drastically reduced which, along with the higher transfer efficiencies, leads to an overall increase in signal-to-noise of 12.4. t_1 noise reduction is further improved with the CSA-free recoupling sequence which yields a signal-to-noise ratio that is 43.1 times higher than $SR4_1^2$, cutting experiment times down by a factor of 1860!

One of the main applications of D-HMQC pulse sequences is for the proton-detection of quadrupolar nuclei. While the central transition of a half-integer quadrupolar nucleus can be inverted with a relatively high fidelity using central transition selective pulses, this efficiency will degrade if we apply hundreds of inversion pulses.[62] We compared the three sequences for $^1H\{^{27}Al\}$ and $^1H\{^{35}Cl\}$ D-HQMC in aluminum acetylacetonate ($Al(acac)_3$) and histidine hydrochloride, respectively. The build-up of the signals is shown in Figures 5a and 6a where we see for the first time that TONE is able to outperform the CSA-free recoupling sequence. While the CSA-free sequence leads to the longest-lived coherences, it yielded the lowest multiple-quantum-filtered signal intensities (Figures 5b and 6b). In a two-dimensional acquisition, however, the performance is much stronger (Figures 5c and 6c). For the $^1H\{^{27}Al\}$ D-HQMC experiments, the CSA-free recoupling sequence yielded a fourfold higher signal-to-noise ratio while TONE improved the signal-to-noise by a factor of 2.3. The results are comparable for the $^1H\{^{35}Cl\}$ D-HQMC experiments wherein the CSA-free sequence improved sensitivity by a factor of 5.0, roughly equal to TONE at 4.7. Note that the two-dimensional spectrum acquired with TONE does seem to have the lower level of noise, which suggests that for a low-γ quadrupolar nuclide like ^{35}Cl, we may expect TONE to yield the highest sensitivity.

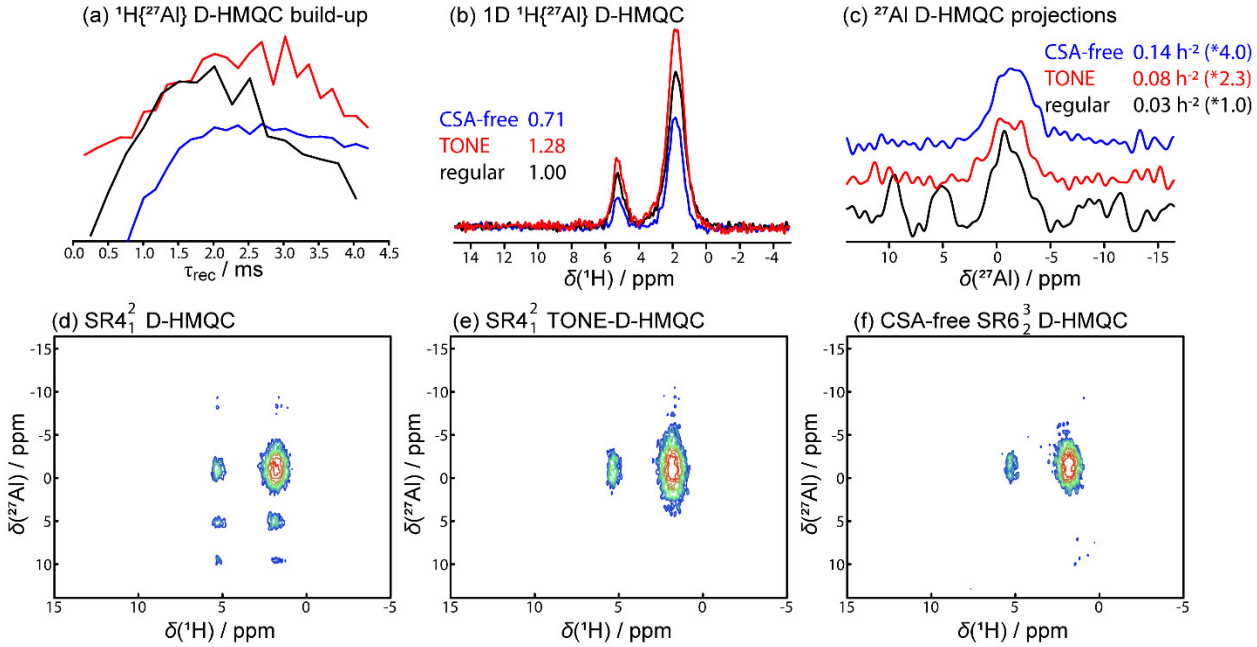

Figure 5. Relative performance of $SR4_1^2$ (black), $SR4_1^2$ with TONE (red), and CSA-free $SR6_2^3$ D-HMQC (blue) sequences in $^1H\{^{27}Al\}$ D-HMQC on Al(acac). The MAS rate was 47.619 kHz. The buildup of signal is shown in (a). The multiple-quantum-filtered ^1H NMR spectra at the optimal

recoupling times are shown in (b). The indirectly-detected ^{27}Al NMR spectra are shown in (c), while the 2D spectra are shown in (d)-(f). Spurious signals in (d) are caused by t_1 noise.

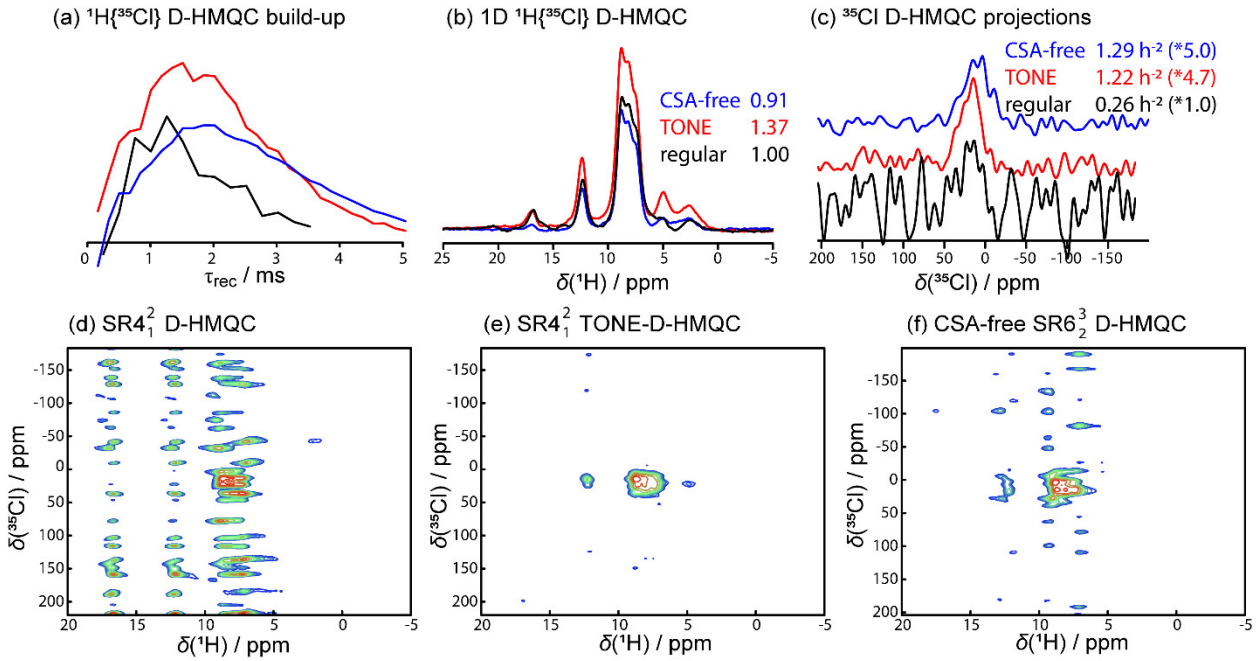

Figure 6. Relative performance of $SR4_1^2$ (black), $SR4_1^2$ with TONE (red), and CSA-free $SR6_2^3$ (blue) D-HMQC sequences in ^{1}H{^{35}Cl} D-HMQC on histidine HCl. The MAS rate was 47.619 kHz. The buildup of signal is shown in (a). The multiple-quantum-filtered ^{1}H NMR spectra at the optimal recoupling times are shown in (b). The indirectly-detected ^{35}Cl NMR spectra are shown in (c), while the 2D spectra are shown in (d)-(f).

The lower performance of the CSA-free sequence for quadrupolar nuclei like ^{27}Al and ^{35}Cl shows that the CSA-free recoupling approach has some strong limitations in cases where the indirectly-detected nuclei are difficult to invert, such as quadrupoles (most notably integer spins) and heavy spin-1/2 nuclei. Note that *a priori* it is not necessary to refocus the CSA every rotor cycle as we have done here. For instance, a sequence with the basic the form: $[(180_{90}180_{270}180_{90})_n(180_{90}180_{270}180_{90})_n]_{0,120,240}$, wherein inversion pulses are applied to the indirect channel every n rotor periods, would also function the same way, however, this would also lengthen the time required for refocusing the ^{1}H homonuclear dipolar interactions and lead to faster decoherence. There may exist a similar recoupling sequence that does not require phase inversion for the refocusing of the homonuclear dipolar interactions, which should outperform all the approaches discussed in this manuscript, however, we were unable to find one.

Conclusions

We have presented a new approach to the zero-quantum recoupling of ^{1}H-X heteronuclear dipolar interactions that is far more robust towards ^{1}H chemical shift anisotropy and spinning instabilities. The recoupling sequence applies $SR6_2^3$ recoupling with a 180_0 basic *R* element. While this symmetry does not recouple *any* anisotropic interactions over its complete 2-rotor period cycle, *m*=1 and 2 heteronuclear dipolar interactions evolve with sizeable scaling factors over single

rotor periods with alternating signs. By applying inversion pulses every rotor period to the second channel, the refocusing of heteronuclear dipolar interactions is prevented while other anisotropic interactions, like the ^{1}H CSA, remain perfectly refocused. The resulting sequence is a continuous, and windowless, TONE-like sequence that leads to remarkable stability relative to MAS fluctuations and very low levels of t_1 noise, when applied in a D-HMQC experiment. In our experiments, the CSA-free $SR6_2^3$ sequence led to 2-43 times higher sensitivity than the traditional D-HMQC sequence, and up to 3.5-fold higher sensitivity than the TONE-D-HMQC approach. For relatively light spin-1/2 nuclei, and half-integer quadrupolar nuclei, this newly presented sequence would appear to be the best choice for maximizing sensitivity, however, the sequence will require modifications to become applicable to other nuclei that are often detected using D-HMQC including integer spins and heavy spin-1/2 nuclei, such as ^{195}Pt.

Materials and Methods

Histidine HCl, aluminum acetylacetonate, and ^{15}N-labelled glycine were all purchased from Aldrich and used as received. The synthesis of the Y-MOF-76 is described in an earlier publication.[63]

NMR Spectroscopy

All experiments were performed on a Bruker AVANCE NEO 600 MHz NMR spectrometer equipped with either a JEOL 0.75 mm MAS probe (glycine) or a PhoenixNMR 1.3 mm MAS probe (Y-MOF-76, histidine HCl, and $Al(acac)_3$). MAS spinning frequencies were set to 83.333 kHz for the experiments performed using 0.75 mm rotors, while the experiments performed using 1.3 mm rotors used an MAS spinning frequency of 47.619 kHz. These MAS frequencies ensured that the recoupling pulses had widths that were multiples of the spectrometer clock for both the $SR4_1^2$ and $SR6_2^3$ sequences. The ^{1}H rf power for non-recoupling pulses was set to 125 and 100 kHz for the 0.75 mm and 1.3 mm rotor experiments, respectively. The ^{15}N, ^{89}Y, ^{27}Al, and ^{35}Cl pulses had effective rf powers of 100, 34, 25, and 50 kHz, respectively. The ^{89}Y and ^{35}Cl rf powers were optimized using the Bloch-Siegert approach as direct detection was impractical.[64]

1D ^{1}H{^{15}N} D-HQMC experiments on ^{15}N-enriched glycine were acquired in 16 scans for the regular and CSA-free sequences, and 20 scans for the TONE sequence, which has a 10-step phase cycle. The recycle delay was set to 1 s for all experiments.

1D ^{1}H{^{89}Y} D-HQMC experiments on Y-MOF-76 were acquired in 1024, 510, and 512 scans for the regular, TONE, and CSA-free sequences, respectively. The 2D spectra were acquired 512, 510, and 512 scans for the regular, TONE, and CSA-free sequences, respectively, and 64 t_1 increments of 105 μs. Totals of 108, 216, and 312 rotor periods of recoupling were applied for the regular, TONE, and CSA-free sequences, respectively, which corresponded to their points of maximum intensity in the 1D measurements. The recycle delay was set to 1 s for all experiments.

1D ^{1}H{^{27}Al} D-HQMC experiments on $Al(acac)_3$ were acquired in 48, 40, and 48 scans for the regular, TONE, and CSA-free sequences, respectively. The 2D spectra were acquired in 16, 20, and 16 scans for the regular, TONE, and CSA-free sequences, respectively, and 64 t_1 increments of 210 μs. Totals of 96, 128, and 128 rotor periods of recoupling were applied for the

regular, TONE, and CSA-free sequences, respectively, which corresponded to their points of maximum intensity in the 1D measurements. The recycle delay was set to 30 s for all experiments.

1D $^{1}H\{^{35}Cl\}$ D-HQMC experiments on Histidine HCl were acquired in 512, 510, and 512 scans for the regular, TONE, and CSA-free sequences, respectively. The 2D spectra were acquired in 64, 60, and 64 scans for the regular, TONE, and CSA-free sequences, respectively, and 80 t_1 increments of 42 μs. The recoupling times lasted 60, 72, and 96 rotor periods for the regular, TONE, and CSA-free sequences, respectively, which corresponded to their optimal recoupling times in the 1D measurements. The recycle delay was set to 4 s for all experiments.

Spin Dynamics Simulations

All spin dynamics calculations were performed using SIMPSON, ver. 4.2.1.[52,53] The spin system was composed of a single ^{1}H and ^{13}C spin pair with a 500 Hz dipolar coupling. The chemical shift tensor anisotropy was set to zero and its orientation was tilted by 90° relative to the principal axis system of the dipolar coupling tensor. Powder averaging was achieved using 232 orientations following the Zaremba-Conroy-Wolfsberg (ZCW) scheme[65-67] and 7 γ angles. The spinning frequency was varied from 49.95 kHz to 50.05 kHz in 1 Hz increments. The recoupling time was incremented from 0 to 15.36 ms in either 240 or 480 μs increments, to ensure the completion of the full supercycles.

Calculations of symmetry-based recoupling sequence scaling factors were performed using SpinDynamica and the Symmetry-Based Recoupling package.[68]

Acknowledgements

This work was supported by the U.S. Department of Energy, Office of Science, Basic Energy Sciences, Materials Science and Engineering Division. The Ames Laboratory is operated for the U.S. DOE by Iowa State University under Contract No. DE-AC02-07CH11358.

Data Availability

All raw experimental spectra and simulated data can be obtained through Zenodo at: 10.5281/zenodo.6612553.

References

[1] A. Pines, M. G. Gibby, J. S. Waugh, Proton-Enhanced NMR of Dilute Spins in Solids, J. Chem. Phys. 59 (1973) 569-590

[2] Y. Ishii, R. Tycko, Sensitivity Enhancement in Solid State ^{15}N NMR by Indirect Detection with High-Speed Magic Angle Spinning, J. Magn. Reson. 142 (2000) 199-204.

[3] J. W. Wiench, C. E. Bronnimann, V. S.-Y. Lin, M. Pruski, Chemical Shift Correlation NMR Spectroscopy with Indirect Detection in Fast Rotating Solids: Studies of Organically Functionalized Mesoporous Silicas. J. Am. Chem. Soc. 129 (2007) 12076-12077.

[4] K. J. Harris, A. Lupulescu, B. E. G. Lucier, L. Frydman, R. W. Schurko, Broadband adiabatic inversion pulses for cross polarization in wideline solid-state NMR spectroscopy, J. Magn. Reson. 224 (2012) 38-47.

[5] A. J. Rossini, M. P. Hanrahan, M. Thuo, Rapid acquisition of wideline MAS solid-state NMR spectra with fast MAS, proton detection, and dipolar HMQC pulse sequences, Phys. Chem. Chem. Phys. 18 (2016) 25284-25295.

[6] J. Koppe, M. Bußkamp, M. R. Hansen, Frequency-Swept Ultra-Wideline Magic-Angle Spinning NMR Spectroscopy, J. Phys. Chem A. 125 (2021) 5643-5649.

[7] A. J. Vega, CP/MAS of quadrupolar $S = 3/2$ nuclei, Solid State Nucl. Magn. Reson. 1 (1992) 17-32.

[8] A. J. Vega, MAS NMR spin locking of half-integer quadrupolar nuclei, J. Magn. Reson. 96 (1992) 50-68.

[9] P. J. Barrie, Distorted powder lineshapes in ^{27}Al CP / MAS NMR spectroscopy of solids, Chem. Phys. Lett. 208 (1993) 486-490.

[10] S. Ding, C. A. McDowell, Theoretical Calculations of the CPMAS Spectral Lineshapes of Half-Integer Quadrupole Systems. J. Magn. Reson. Ser. A. 114 (1995) 80-87.

[11] L. H. Merwin, A. Sebald, The First ^{89}Y CP-MAS Spectra, J. Magn. Reson. 88 (1990) 167-171.

[12] L. H. Merwin, A. Sebald, The First Examples of ^{109}Ag CP MAS Spectroscopy, J. Magn. Reson. 97 (1992) 628-631.

[13] C. Martineau, B. Bouchevreau, F. Taulelle, J. Trébosc, O. Lafon, J.-P. Amoureux, High-resolution through-space correlations between spin-1/2 and half-integer quadrupolar nuclei using the MQ-D-R-INEPT NMR experiment, Phys. Chem. Chem., Phys. 14 (2012) 7112-7119.

[14] X. Zhao, W. Hoffbauer, J. S. Auf. der Günne, M. H. Levitt, Heteronuclear polarization transfer by symmetry-based recoupling sequences in solid-state NMR, Solid State Nucl. Magn. Reson. 26 (2004) 57-64.

[15] G. Tricot, J. Trébosc, F. Pourpoint, R. Gauvin, L. Delevoye, Chapter Four - The D-HMQC MAS-NMR Technique: An Efficient Tool for the Editing of Through-Space Correlation Spectra Between Quadrupolar and Spin-1/2 (31P, 29Si, 1H, 13C) Nuclei, Annu. Rep. NMR Spectrosc. 81 (2014) 145-184.

[16] M. Taoufik, K. C. Szeto, N. Merle, I. Del Rosal, L. Maron, J. Trébosc, G. Tricot, R. Gauvin, L. Delevoye, Heteronuclear NMR Spectroscopy as a Surface-Selective Technique: A Unique Look at the Hydroxyl Groups of γ-Alumina, Chem. Eur. J. 20 (2014) 4038-4046.

[17] F. A. Perras, T. Kobayashi, M. Pruski, Natural Abundance ^{17}O DNP Two-Dimensional and Surface-Enhanced NMR Spectroscopy, J. Am. Chem. Soc. 137 (2015) 8336-8339.

[18] F. A. Perras, T. Kobayashi, M. Pruski, PRESTO polarization transfer to quadrupolar nuclei: implications for dynamic nuclear polarization, Phys. Chem. Chem. Phys. 17 (2015) 22616-22622.

[19] A. Venkatesh, M. P. Hanrahan, A. J. Rossini, Proton detection of MAS solid-state NMR spectra of half-integer quadrupolar nuclei, Solid State Nucl. Magn. Reson. 84 (2017) 171-181.

[20] H. Nagashima, A. S. L. Thankamony, J. Trébosc, F. Pourpoint, O. Lafon, J.-P. Amoureux, γ-Independent through-space hetero-nuclear correlation between spin-1/2 and quadrupolar nuclei in solids, Solid State Nucl. Magn. Reson. 84 (2017) 216-226.

[21] H. Nagashima, J. Trébosc, Y. Kon, K. Sato, O. Lafon, J.-P. Amoureux, Observation of Low-γ Quadrupolar Nuclei by Surface-Enhanced NMR Spectroscopy, J. Am. Chem. Soc. 142 (2020) 10659-10672.

[22] A. Venkatesh, A. Lund, L. Rochlitz, R. Jabbour, C. P. Gordon, G. Menzildjian, J. Viger-Gravel, P. Berruyer, D. Gajan, C. Copéret, A. Lesage, A. J. Rossini, The Structure of Molecular and Surface Platinum Sites Determined by DNP-SENS and Fast MAS ^{195}Pt Solid-State NMR Spectroscopy, J. Am. Chem. Soc. 142 (2020) 18936-18945.

[23] T. Kobayashi, M. Pruski, Indirectly Detected DNP-Enhanced ^{17}O NMR Spectroscopy: Observation of Non-Protonated Near-Surface Oxygen at Naturally Abundant Silica and Silica-Alumina, ChemPhysChem. 22 (2021) 1441-1445.
[24] Z. Gan, ^{13}C/^{14}N heteronuclear multiple-quantum correlation with rotary resonance and REDOR dipolar recoupling, J. Magn. Reson. 184 (2007) 39-43.
[25] O. Lafon, Q. Wang, B. Hu, F. Vasconcelos, J. Trébosc, S. Cristol, F. Deng, J.-P. Amoureux, Indirect Detection via Spin-1/2 Nuclei in Solid State NMR Spectroscopy: Application to the Observation of Proximities between Protons and Quadrupolar Nuclei, J. Phys. Chem. A. 113 (2009) 12864-12878.
[26] A. Venkatesh, F. A. Perras, A. J. Rossini, Proton-detected solid-state NMR spectroscopy of spin-1/2 nuclei with large chemical shift anisotropy, J. Magn. Reson. 327 (2021) 106983.
[27] J. Trébosc, O. Lafon, B. Hu, J.-P. Amoureux, Indirect high-resolution detection for quadrupolar spin-3/2 nuclei in dipolar HMQC solid-state NMR experiments, Chem. Phys. Lett. 496 (2010) 201-207.
[28] A. S. Tatton, T. N. Pham, F. G. Vogt, D. Iuga, A. J. Edwards, S. P. Brown, Probing Hydrogen Bonding in Cocrystals and Amorphous Dispersions Using ^{14}N–^{1}H HMQC Solid-State NMR, Mol. Pharmaceutics. 10 (2013) 999-1007.
[29] Q. Wang, Y. Li, J. Trébosc, O. Lafon, J. Xu, B. Hu, N. Feng, Q. Chen, J.-P. Amoureux, F. Deng, Population transfer HMQC for half-integer quadrupolar nuclei, J. Chem. Phys. 142 (2015) 094201.
[30] F. A. Perras, A. Venkatesh, M. P. Hanrahan, T. W. Goh, W. Huang, A. J. Rossini, M. Pruski, Indirect detection of infinite-speed MAS solid-state NMR spectra, J. Magn. Reson. 276 (2017) 95-102.
[31] A. Venkatesh, M. P. Hanrahan, A. J. Rossini, Proton detection of MAS solid-state NMR spectra of half-integer quadrupolar nuclei, Solid State Nucl. Magn. Reson. 84 (2017) 171-181.
[32] N. T. Duong, Z. Gan, Y. Nishiyama, Selective ^{1}H-^{14}N Distance Measurements by ^{14}N Overtone Solid-State NMR Spectroscopy at Fast MAS, Front. Mol. Biosci. 8 (2021) 645347.
[33] D. Iuga, E. K. Corlett, S. P. Brown, ^{35}Cl–^{1}H Heteronuclear correlation magic-angle spinning nuclear magnetic resonance experiments for probing pharmaceutical salts, Magn. Reson. Chem. 59 (2021) 1089-1100.
[34] M. H. Levitt, Symmetry-based pulse sequences in magic angle spinning solid-state NMR, Encyclopedia of Magnetic Resonance, 9 (2002) 165-196.
[35] I. Hung, Z. Gan, High-Resolution NMR of S = 3/2 Quadrupole Nuclei by Detection of Double-Quantum Satellite Transitions via Protons, J. Phys. Chem. Lett. 11 (2020) 4734-4740.
[36] R. Bayzou, J. Trébosc, I. Hung, Z. Gan, O. Lafon, J.-P. Amoureux, Indirect NMR detection via proton of nuclei subject to large anisotropic interactions, such as ^{14}N, ^{195}Pt, and ^{35}Cl, using the T-HMQC sequence, J. Chem. Phys. 156 (2022) 064202.
[37] A. Venkatesh, X. Luan, F. A. Perras, I. Hung, W. Huang, A. J. Rossini, t_1-Noise eliminated dipolar heteronuclear multiple-quantum coherence solid-state NMR spectroscopy, Phys. Chem. Chem. Phys. 22 (2020) 20815-20828.
[38] B. A. Atterberry, S. L. Carnahan, Y. Chen, A. Venkatesh, A. J. Rossini, Double echo symmetry-based REDOR and RESPDOR pulse sequences for proton detected measurements of heteronuclear dipolar coupling constants, J. Magn. Reson. 336 (2022) 107147.
[39] A. Brinkmann, M. H. Levitt, Symmetry principles in the nuclear magnetic resonance of spinning solids: Heteronuclear recoupling by generalized Hartmann–Hahn sequences, J. Chem. Phys. 115 (2001) 357-384.

[40] T. Gullion, J. Schaefer, Rotational-echo double-resonance NMR, J. Magn. Reson. 81 (1989) 196-200.
[41] J. R. Garbow, T. Gullion, The importance of precise timing in pulsed, rotor-synchronous MAS NMR, Chem. Phys. Lett. 192 (1992) 71-76.
[42]S. V. Dvinskikh, H. Zimmermann, A. Maliniak, D. Sandström, Measurements of motionally averaged heteronuclear dipolar couplings in MAS NMR using R-type recoupling, J. Magn. Reson. 168 (2004) 194-201.
[43] G. Hou, X. Lu, A. J, Vega, T. Polenova, Accurate measurement of heteronuclear dipolar couplings by phase-alternating R-symmetry (PARS) sequences in magic angle spinning NMR spectroscopy, J. Chem. Phys. 141 (2014) 104202.
[44] M. Carravetta, M. Edén, X. Zhao, A. Brinkmann, M. H. Levitt, Symmetry principles for the design of radiofrequency pulse sequences in the nuclear magnetic resonance of rotating solids, Chem. Phys. Lett. 321 (2000) 2005-215.
[45] A. Brinkmann, J. S. auf der Günne, M. H. Levitt, Homonuclear Zero-Quantum Recoupling in Fast Magic-Angle Spinning Nuclear Magnetic Resonance, J. Magn. Reson. 156 (2002) 79-96.
[46] A. Brinkmann, A. P. M. Kentgens, Proton-Selective ^{17}O-^{1}H Distance Measurements in Fast Magic-Angle-Spinning Solid-State NMR Spectroscopy for the Determination of Hydrogen Bond Lengths, J. Am. Chem. Soc. 128 (2006) 14758-14759.
[47] A. Brinkmann, A. P. M. Kentgens, Sensitivity Enhancement and Heteronuclear Distance Measurements in Biological ^{17}O Solid-State NMR, J. Phys. Chem. B. 110 (2006) 16089-16101.
[48] A. Brinkmann, M. Edén, M. H. Levitt, Synchronous helical pulse sequences in magic-angle spinning nuclear magnetic resonance: Double quantum recoupling of multiple-spin systems, J. Chem. Phys. 112 (2000) 8539-8554.
[49] A. Brinkmann, M. Edén, Second order average Hamiltonian theory of symmetry-based pulse schemes in the nuclear magnetic resonance of rotating solids: Application to triple-quantum dipolar recoupling, J. Chem. Phys. 120 (2004) 11726-11745.
[50] P. E. Kristiansen, M. Carravetta, J. D. van Beek, W. C. Lai, M. H. Levitt, Theory and applications of supercycled symmetry-based recoupling sequences in solid-state nuclear magnetic resonance, J. Chem. Phys. 124 (2006) 234510.
[51] M. Edén, Order-selective multiple-quantum excitation in magic-angle spinning NMR: creating triple-quantum coherences with a trilinear Hamiltonian, Chem. Phys. Lett. 366 (2002) 469-476.
[52] M. Bak, J. T. Rasmussen, N. C. Nielsen, SIMPSON: A General Simulation Program for Solid-State NMR Spectroscopy, J. Magn. Reson. 147 (2000) 296-330.
[53] Z. Tošner, R. Andersen, B. Stevensson, M. Edén, N. C. Nielsen, T. Vosegaard, Computer-intensive simulation of solid-state NMR experiments using SIMPSON, J. Magn. Reson. 246 (2014) 79-93.
[54] T. Gullion, D. B. Baker, M. S. Conradi, New Compensated Carr-Purcell Sequences, J. Magn. Reson. 89 (1990) 479-484.
[55] Y. Nishiyama, R. Zhang, A. Ramamoorthy, Finite-pulse radio frequency driven recoupling with phase cycling for 2D ^{1}H/^{1}H correlation at ultrafast MAS frequencies, J. Magn. Reson. 243 (2014) 25-32.
[56] A. J. Shaka, S. P. Rucker, A. Pines, Iterative Carr-Purcell Trains, J. Magn. Reson. 77 (1988) 606-611.
[57] G. N. B. Yip, E. R. P. Zuiderweg, A phase cycle scheme that significantly suppresses offset-dependent artifacts in the R_2-CPMG ^{15}N relaxation experiment, J. Magn. Reson. 171 (2004) 25-36.

[58] V. S. Manu, G. Veglia, Genetic algorithm optimized triply compensated pulses in NMR spectroscopy, J. Magn. Reson. 260 (2015) 136-143.
[59] H.-L. Jian, N. Tsumori, Q. Xu, A series of (6,6)-connected porous lanthanide-organic framework enantiomers with high thermostability and exposed metal sites: scalable syntheses, structures, and sorption properties, Inorg. Chem. 49 (2010) 10001-10006.
[60] J. Luo, H. Xu, Y. Liu, Y. Zhao, L. L. Daemen, C. Brown, T.V. Timofeeva, S. Ma, H.-C. Zhou Hydrogen adsorption in a highly stable porous rare-earth metal-organic framework: sorption properties and neutron diffraction studies, J. Am. Chem. Soc. 130 (2008) 9626-9627.
[61] N.L. Rosi, J. Kim, M. Eddaoudi, B. Chen, M. O'Keefe, O.M. Yaghi. Rod Packings and Metal-Organic Frameworks Constructed from Rod-Shaped Secondary Building Units, J. Am. Chem. Soc. 127 (2005) 1504-1518.
[62] D. Jardón-Alvarez, M. O. Bovee, J. H. Baltisberger, P. J. Grandinetti, Natural abundance ^{17}O and ^{33}S nuclear magnetic resonance spectroscopy in solids achieved through extended coherence lifetimes, Phys. Rev. B. 100 (2019) 140103.
[63] F. A. Perras, T. W. Goh, L.-L. Wang, W. Huang, M. Pruski, Enhanced ^{1}H-X D-HMQC performance through improved ^{1}H homonuclear decoupling, Solid State Nucl. Magn. Reson. 98 (2019) 12-18.
[64] I. Hung, P. Gor'kov, Z. Gan, Using the heteronuclear Bloch-Siegert shift of protons for B_1 calibration of insensitive nuclei not present in the sample, J. Magn. Reson. 310 (2020) 106636.
[65] S. K. Zaremba, Good lattice points, discrepancy, and numerical integration, Ann. Mat. Pura Appl. 73 (1966) 293-317.
[66] H. Conroy, Molecular Schrödinger Equation. VIII. A New Method for the Evaluation of Multidimensional Integrals, J. Chem. Phys. 47 (1967) 5307-5318.
[67] V. B. Chang, H. H. Suzukawa, M. Wolfsberg, Investigations of a nonrandom numerical method for multidimensional integration, J. Chem. Phys. 59 (1973) 3992-3999.
[68] C. Bengs, M. H. Levitt, SpinDynamica: Symbolic and numerical magnetic resonance in a Mathematica environment, Magn. Reson. Chem. 56 (2018) 374-414.